

“Melting and solidification of binary alloy subjected to cyclic temperature and heat flux boundary condition”

A project report submitted in partial fulfillment of the requirements for
the degree of

**Bachelor of Technology
in
Mechanical Engineering**

By

**SUBHRANSU KUMAR MISHRA
Roll -10503001**

**Under the guidance of
Prof. Prasenjit Rath**



DEPARTMENT OF MECHANICAL ENGINEERING
NATIONAL INSTITUTE OF TECHNOLOGY
ROURKELA
2008-09



NATIONAL INSTITUTE OF TECHNOLOGY, ROURKELA

CERTIFICATE

This is to certify that the project report entitled “**Melting and solidification of binary alloy subjected to cyclic temperature and heat flux boundary condition**” by **Subhransu Kumar Mishra**, has been carried out under my supervision in partial fulfillment of the requirement for the degree of **Bachelor of Technology in Mechanical Engineering** during the session 2008-09 in the Department of Mechanical Engineering, National Institute of Technology, Rourkela and this work has not been submitted elsewhere for a degree.

Place: Rourkela
Date:

Prof. Prasenjit Rath
Mechanical Engineering Dept.
N.I.T, Rourkela

Acknowledgement

I wish to express my heartfelt thanks and deep sense of gratitude to Prof Prasenjit Rath for his excellent guidance and whole hearted involvement during the project work. I am also indebted to him for his encouragement, affection and moral support throughout the project. I am also thankful to him for his valuable time he has provided with the practical guidance at every step of the project work.

I would also like to thank my family and friends who have been a constant source of inspiration and encouragement during the entire period and lastly everyone else who directly or indirectly helped me in this project work.

Date:

Subhransu Kumar Mishra
Mechanical Engineering Dept.
N.I.T, Rourkela

ABSTRACT

An enthalpy based Fixed-Grid method is developed for modeling phase change in a binary alloy subjected to periodic boundary condition. A two-dimensional model is developed for the melting and solidification cycle a gallium-tin (eutectic) alloy. The model also includes the natural convection effect in the liquid zone. Two cases are studied: (1) one of the boundaries is subjected to periodic variation of the temperature and (2) the same boundary subjected to periodic variation of heat flux. An enthalpy based fixed grid approach is used to solve the energy equation. The SIMPLER algorithm of Patankar is used to calculate the flow variables from continuity and momentum equations. The Tri-Diagonal-Matrix-Algorithm is used to solve the algebraic discrete equations. The melting and solidification fronts are captured implicitly by calculating the latent heat content at each control volume. An iterative update procedure is developed to update the latent heat content at each control volume. The proposed methodology is very simple to implement as the grid size is fixed. Since the grid size is fixed, hence the computational domain is also fixed. The domain is discretized once at the beginning of computation. The results obtained using the proposed enthalpy method is being validated with the available experimental results for melting of pure gallium. It is seen that, the solidification front takes a rather more regular shape, than the melting front. This is because of the rapid dissipation of temperature gradients in the melt. Hence, the movement of the solidification front is not modified by the fluid flow.

TABLE OF CONTENT

<u>Content</u>	<u>Page No</u>
CERTIFICATE	1
ACKNOWLEDGEMENT	2
ABSTRACT	3
NOMENCLATURE	5
CHAPTER 1: INTRODUCTION	7
CHAPTER 2: LITERATURE SURVEY	10
i. Derivation of Stefan's condition	12
ii. Linear phase change alloys	16
CHAPTER 3: PROBLEM DESCRIPTION	19
CHAPTER 4: MATHEMATICAL MODELLING	22
i. The governing equations	23
ii. The enthalpy update procedure	26
iii. Numerical method	27
CHAPTER 5: MODEL VALIDATION	29
CHAPTER 6: RESULTS AND DISCUSSION	34
CHAPTER 7: CONCLUSION	40
CHAPTER 8: REFERENCES	42

Nomenclature

a	coefficient of the discretization equation
C	specific heat of the material
f	liquid fraction
g	acceleration due to gravity (9.81 m/s^2)
H	total enthalpy
K	thermal conductivity of the material
L	latent heat
T	temperature
T_{pc}	phase change temperature
T_s	solidous temperature
T_l	liquidous temperature
t	time
u, v	liquid metal velocity in x - and y -directions
x, y	coordinate directions

Greek Symbols

α	thermal diffusivity
β	thermal expansion coefficient
λ	under-relaxation factor
ρ	density of the material
Δt	time step

ΔH latent heat content of the material

Subscripts

m melting

P control volume P

o initial time ($t = 0$)

Superscripts

n iteration number

o previous time step

CHAPTER 1

INTRODUCTION:

Cyclic heat addition and removal from a phase change material involves a multiphase, simultaneous melting and solidification process, which finds applications in electronic chip cooling, energy storage and food processing treatment among others. Successive solidification and melting of a region driven by a boundary temperature that cycles above and below the solid/liquid phase change temperature. The cyclic boundary condition makes this phenomenon more interesting as there is re-melting and re-solidification phenomena due to the oscillation in temperature in the vicinity of its melting temperature. Analysis of heat transfer in this process involves the study of a special kind of moving boundary problem where the position of the moving boundary is priori an unknown. This is otherwise known as the Stefan problem. An additional condition is required to predict the position and shape of the interface which is known as the interface or Stefan condition obtained from the energy balance at the solid-liquid interface. It is difficult to solve the Stefan problem because of the unknown moving boundary. Further, the problem will be more difficult to solve especially when one of the boundaries is imposed with cyclic variation of temperature that cycles above and below the melting/solidification temperature due to the simultaneous evolution of multiple moving boundaries. During the heating phase of the cycle, the medium melts and the melting front moves from the surface to the interior of the body. Next, during the cooling phase of the cycle, the melted region near the boundary surface (imposed with cyclic variation of temperature) re-solidified and a solidification front also appears. There are two phase change fronts in the medium. It is interesting to make an analysis whether the second solidification front is able to catch up the first melt front and how heat is stored in different phases of the medium. This depends greatly on the imposed cyclic condition in the boundary surface and the latent heat content of the material. It is impossible to solve this problem exactly [1-7]. This is an **isothermal** case for a substance having a definite melting point, however for an alloy, which is the mixture of 2 or more melts, there exists no definite melting point. An alloy in solid state softens over a range of temperatures before finally melting. The analysis of this type **non-isothermal** problems is more difficult of the presence of the **mushy zone**. It is impossible to solve the problems analytically, however approximate solutions are possible and these problems poses a real challenge to accurate analysis

Approximate analytical solution methods for the solution of Stefan problem is the power series method [8]. However, it is associated with severe limitations like isothermal interface, constant properties, etc. which is discussed detail in Duda and Vrentas [9]. The two well known numerical methods to solve this kind of moving boundary problem are the moving grid (MG) method and the fixed grid (FG) method. Hasan [10] uses MG approach, Gong et al. [11] used a FG based enhanced heat capacity methods and Brent et al. [12] developed an enthalpy based FG method for modeling solid-liquid phase change process involving melting of pure metal. Voller et al. [13] developed an enthalpy porosity based FG method for cyclic phase change with imposed periodic variation of temperature at the boundary. Overall, the MG method is an explicit approach for tracking the solid-liquid interface. The interface is displaced at a certain instant of time by using the interface condition explicitly. Extension of MG approach to multidimensional phase change requires unstructured mesh system which needs an efficient mesh generation tool. Hence, computationally MG approach is very expensive. In contrast, enthalpy based FG method is an implicit approach for tracking the moving interface. The moving interface is captured through a order parameter known as the latent heat content. It is very easy to extend this method for multidimensional phase change problems as it is based on simple Cartesian grid which is easy to generate.

From the critical literature survey, it is found that very limited study is being conducted in the phase change process subjected to fluctuating boundary conditions. Although Choi and Hsieh [8] introduced this kind of phase change problem, but it was limited to one-dimensional (1-D) analysis. Later, Voller et al. [13] have developed a two-dimensional (2-D) model under fluctuating temperature boundary condition.

In this paper, an enthalpy based fixed grid method is used to model the two dimensional (2-D) simultaneous melting and solidification of a binary alloy subjected to periodic variation of temperature and heat flux at one of the boundaries described in the next section. An appropriate mathematical model is then briefly described based on the single equation enthalpy approach. A brief description of the numerical method is then follows. The overall solution procedure is described next. Then, finally, few results are discussed followed by conclusions.

CHAPTER 2

LITERATURE SURVEY:

Derivation of the Stefan's condition taking case of melting of ice

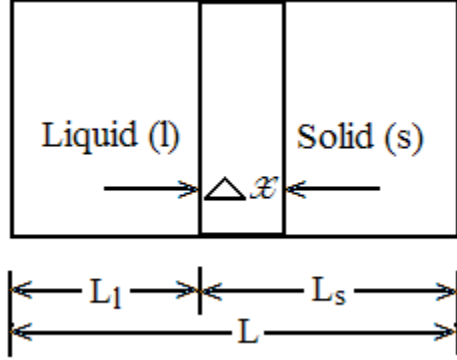


Fig 1

Governing enthalpy equation:

$$\frac{\partial(\rho H)}{\partial t} = \frac{\partial}{\partial x} \left(K \frac{\partial T}{\partial x} \right) \quad (1)$$

At time (t),

$$\begin{aligned} \int_0^L \rho H dx &= \int_0^{L_l} (\rho H)_l dx + \int_{L_l}^L (\rho H)_s dx \\ \Rightarrow \int_0^L \rho H dx &= \int_0^{L_l} (\rho H)_l dx + \int_{L_l}^{L_l+\Delta x} (\rho H)_s dx + \int_{L_l+\Delta x_l}^L (\rho H)_s dx \end{aligned} \quad (2)$$

and at time $(t + \Delta t)$,

$$\begin{aligned} \int_0^L \rho H dx &= \int_0^{L_l+\Delta x} (\rho H)_l dx + \int_{L_l+\Delta x}^L (\rho H)_s dx \\ \Rightarrow \int_0^L \rho H dx &= \int_0^{L_l} (\rho H)_l dx + \int_{L_l}^{L_l+\Delta x} (\rho H)_l dx + \int_{L_l+\Delta x_l}^L (\rho H)_s dx \end{aligned} \quad (3)$$

Subtracting Eq.(2) from Eq.(3), dividing by Δt , and taking limits as $\Delta t \rightarrow 0$

$$\begin{aligned}
\frac{d}{dt} \int_0^L \rho H dx &= \frac{d}{dt} \int_0^{L_l} (\rho H)_l dx + \frac{d}{dt} \int_{L_l+\Delta x}^L (\rho H)_s dx \\
&+ \lim_{\Delta t \rightarrow 0} \int_{L_l}^{L_l+\Delta x} \frac{(\rho H)_{l,t+\Delta t} - (\rho H)_{s,t}}{\Delta t} dx
\end{aligned} \tag{4}$$

Expanding the integral in the left side of the Eq.(4), gives

$$\frac{d}{dt} \int_0^L \rho H dx = \frac{d}{dt} \int_0^{L_l} (\rho H)_l dx + \frac{d}{dt} \int_{L_l}^{L_l+\Delta x} \rho H dx + \frac{d}{dt} \int_{L_l+\Delta x}^L (\rho H)_s dx \tag{5}$$

Solving Eq.(4) and Eq.(5), we get

$$\frac{d}{dt} \int_{L_l}^{L_l+\Delta x} \rho H dx = \lim_{\Delta t \rightarrow 0} \int_{L_l}^{L_l+\Delta x} \frac{(\rho H)_{l,t+\Delta t} - (\rho H)_{s,t}}{\Delta t} dx \tag{6}$$

Using the relations as given in Eq.(1), Eq.(6) can be written as

$$\begin{aligned}
\int_{L_l}^{L_l+\Delta x} \frac{\partial}{\partial x} \left(K \frac{\partial T}{\partial x} \right) dx &= \lim_{\Delta t \rightarrow 0} \int_{L_l}^{L_l+\Delta x} \frac{(\rho H)_{l,t+\Delta t} - (\rho H)_{s,t}}{\Delta t} dx \\
\Rightarrow k_s \frac{\partial T_s}{\partial x} - k_l \frac{\partial T_l}{\partial x} &= \lim_{\Delta t \rightarrow 0} \int_{L_l}^{L_l+\Delta x} \frac{(\rho H)_{l,t+\Delta t} - (\rho H)_{s,t}}{\Delta t} dx
\end{aligned}$$

Remembering that as $\Delta t \rightarrow 0$, $L_l + \Delta x \rightarrow L_l$. Simultaneously, H_s and H_l approach their saturation values H_s^* and H_l^* and the ratio $\partial x / \Delta t$ approaches v_{ns} , where v_{ns} is the local velocity of the interfacial surface elements towards the solid region. Hence the above equation can be simplified as

$$k_s \frac{\partial T_s}{\partial x} - k_l \frac{\partial T_l}{\partial x} = \rho (H_l^* - H_s^*) v_{ns} \tag{7}$$

Now,

$$H_s^*(t) = C_p T_m + 0$$

And

$$H_l^* - H_s^* = L$$

Where L is the enthalpy of fusion or the latent heat of fusion. It is the amount of heat added to ice per unit mass to completely convert it to liquid. Therefore, Eq.(7) can be written as

$$k_s \frac{\partial T_s}{\partial x} - k_l \frac{\partial T_l}{\partial x} = \rho L v_{nl} \quad (8)$$

Eq.(7) is the required interface condition in solidification or melting problems.

The Enthalpy Method

The enthalpy is the heat content of a system. The basic idea is to represent the enthalpy of a system as a sum of the sensible and latent heat content

$$H = h + \Delta H \quad (9)$$

Where H=Total Enthalpy

h=Sensible Enthalpy

ΔH =Latent Heat

The sensible heat is a function of the temperature and its value is given by $C_p T$. The Latent heat is not a function of temperature in case of isothermal phase change. The latent heat is constrained by $0 \leq \Delta H \leq L$

Liquid Fraction:

$$\frac{\Delta H}{L}$$

Solid Fraction:

$$1 - \frac{\Delta H}{L}$$

Relation between the latent heat content and the temperature for

Isothermal case:

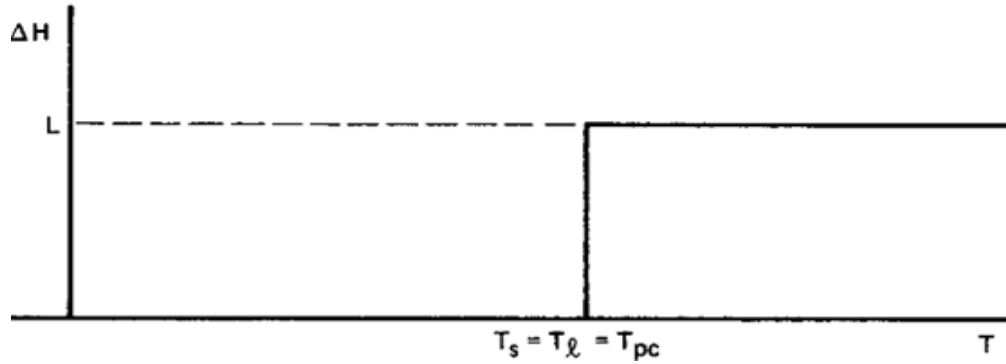


Fig. 1 Relation between ΔH and T for isothermal case [19]

Non-Isothermal (Generalized)

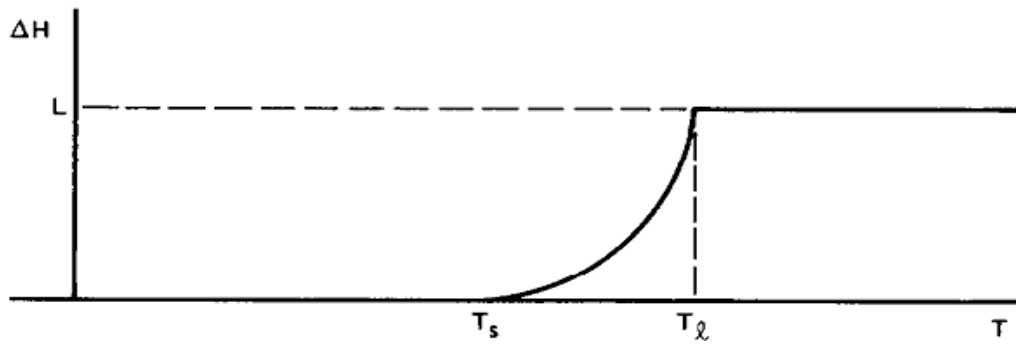


Fig. 2 Relation between ΔH and T for generalized case [19]

Non-Isothermal (Linear phase change)

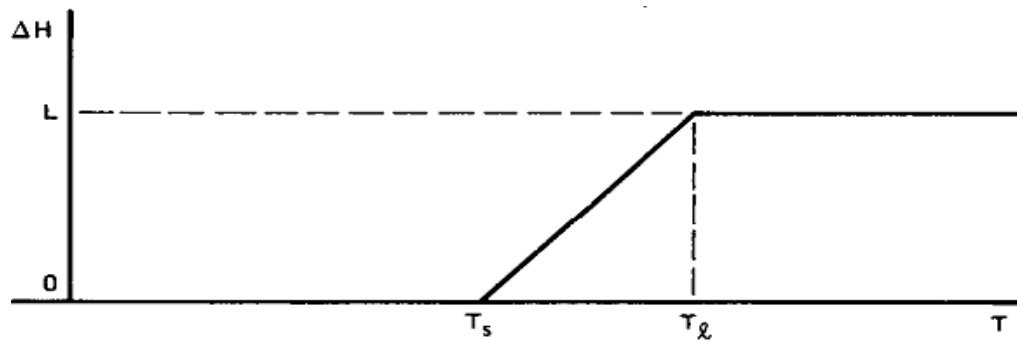


Fig. 3 Relation between ΔH and T for Linear phase change case [19]

Linear Phase Change alloys

The linear phase change alloys have no definite melting point. They soften over a range of temperature

T_s =Solidous Temperature

T_l =Liquidous Temperature

T_{pc} =Phase change Temperature= $(T_s + T_l)/2$

Relation Between ΔH and h for linear phase change alloy

$$\Delta H = Ah + B \quad (10)$$

$$0 = AC_p T_s + B \quad (11)$$

$$L = AC_p T_l + B \quad (12)$$

$$A = \frac{L}{C_p(T_l - T_s)} \quad (13)$$

$$B = \frac{-LT_s}{(T_l - T_s)} \quad (14)$$

$$T_{pc} = \frac{1}{2}(T_l + T_s) \quad (15)$$

$$\varepsilon = \frac{1}{2}(T_l - T_s) \quad (16)$$

$$\Delta H = \frac{L}{2\varepsilon}[T - T_{pc} + \varepsilon] \quad (17)$$

$$\frac{2\varepsilon C_p \Delta H}{L} = C_p T - C_p T_{pc} + C_p \varepsilon \quad (18)$$

$$h = \frac{\varepsilon C_p}{L}(2\Delta H - \Delta L) + C_p T_{pc} \quad (19)$$

$$h = f^{-1}(\Delta H) \quad (20)$$

$$\Delta H = f(h) \quad (21)$$

Governing Equation

$$\nabla \cdot (\rho u H) = \nabla \cdot \left(\frac{K}{C_p} \nabla H \right) \quad (22)$$

$$H = h + \Delta H \quad (23)$$

Substituting in above equation we have

$$(\nabla \cdot (\rho u h)) = \nabla \cdot \left(\frac{K}{C_p} \nabla h \right) - \nabla \cdot (\rho u \Delta H) \quad (24)$$

The last term is the source term S

$$S = -\nabla \cdot (\rho u \Delta H) \quad (25)$$

The discretization is done using the finite volume method. In such an approach, the discretization equations are obtained by applying conservation laws over finite size control volumes surrounding the grid nodes

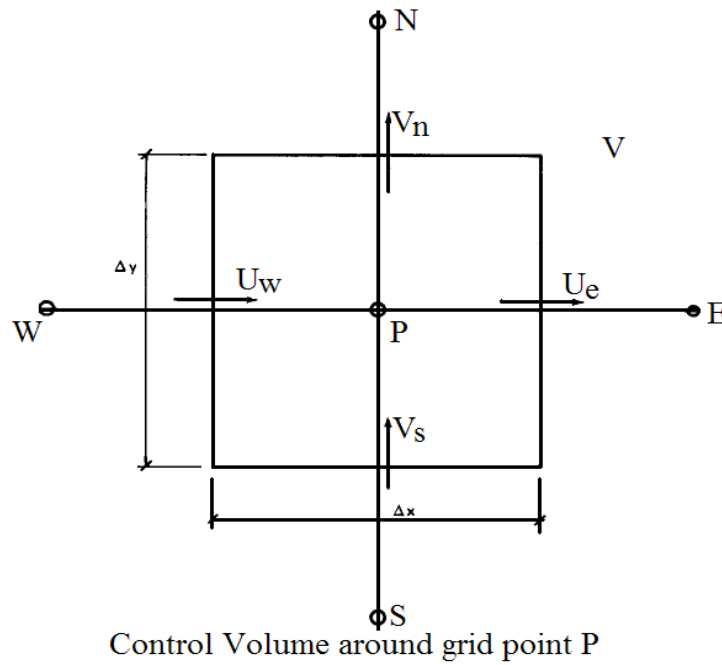


Fig. 4

$$\begin{aligned}
& \int_s^n \int_w^e (\nabla \cdot (\rho u h) dx) dy \\
&= \int_s^n \int_w^e (\nabla \cdot \left(\frac{K}{C_p} \nabla h \right) dx) dy - \int_s^n \int_w^e (\nabla \cdot (\rho u \Delta H) dx) dy
\end{aligned} \tag{26}$$

Solving and discretizing the above equation using the finite difference method we have

The integration of the third term gives us

$$(\rho u)_w \Delta y (\Delta H)_w + (\rho v)_s \Delta x (\Delta H)_s - (\rho u)_e \Delta y (\Delta H)_e - (\rho v)_n \Delta x (\Delta H)_n \tag{27}$$

This term contains the ΔH field which is required to know the h field. So an iterative procedure has been developed for the solution of h and ΔH

1. Let $(\Delta H)^k$ represent the (ΔH) field as it exists at the beginning of the k^{th} iteration.
2. Using $(\Delta H)^k$ to compute the source term S , solve the governing equation to obtain h^k
3. Finally obtain $(\Delta H)^{k+1}$, the (ΔH) field for the next

iteration, using

$$\Delta H^{k+1} = \Delta H^k + h^k - f^{-1}(\Delta H^k) \tag{28}$$

Substituting the value of

$$h = f^{-1}(\Delta H) \tag{29}$$

we have

$$\Delta H^{k+1} = \Delta H^k + h^k - \frac{C_p \varepsilon}{L} (2\Delta H^k - L) - C_p T_{pc} \tag{30}$$

$$0 \leq \Delta H^{k+1} \leq L$$

CHAPTER 3

PROBLEM DESCRIPTION:

Melting and solidification in a 2-D rectangular gallium-tin (eutectic) alloy cavity is taken to study the influence of fluctuating temperature cycles around the melting temperature on the phase front evolution. The schematic and the computational domain is shown in Fig. 5. Two cases are discussed in this paper: one with imposed cyclic variation of temperature (shown in Fig. 5a) and another with imposed cyclic variation of heat flux (shown in Fig. 5b). Three sides of the cavity are insulated and the left boundary is imposed with cyclic variation of temperature and heat flux. The proposed model accounted for the natural convection effect in the melt zone. The following important assumptions are made in developing the mathematical model for this phase change problem.

1. The thermal properties of the material are assumed constant.
2. The density of solid and liquid phase is assumed to be same.
3. Boussinesq approximation is used for treating the buoyancy term in the momentum equation.

Property	Value
Specific heat capacity (C)	409.58 J/kg-K
Thermal expansion coefficient (β)	$1.3054 \times 10^{-4} \text{ K}^{-1}$
Thermal diffusivity (α)	$1.4145 \times 10^{-5} \text{ m}^2/\text{s}$
Latent heat (L)	80160 J/kg
Phase change temperature (T_{pc})	0K
Kinematic viscosity (ν)	$2.97 \times 10^{-7} \text{ m}^2/\text{s}$

Table 1: Properties of gallium-tin alloy.

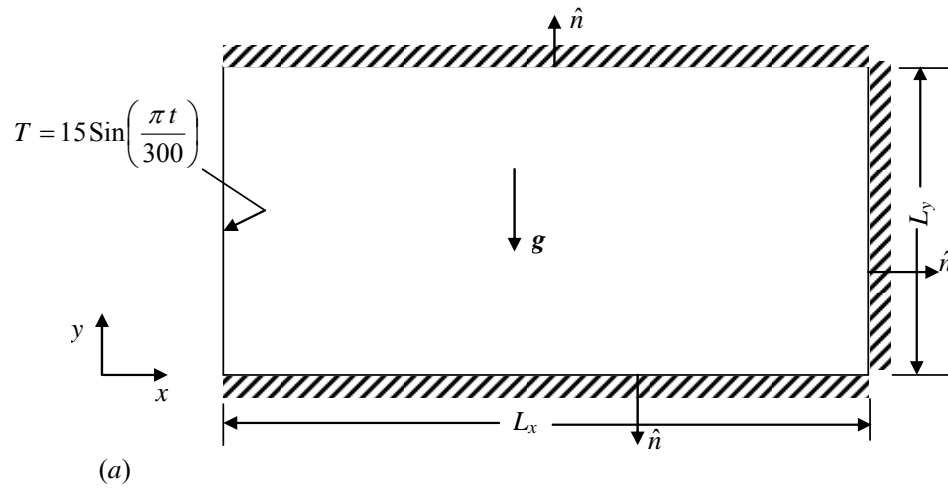


Fig. 5a

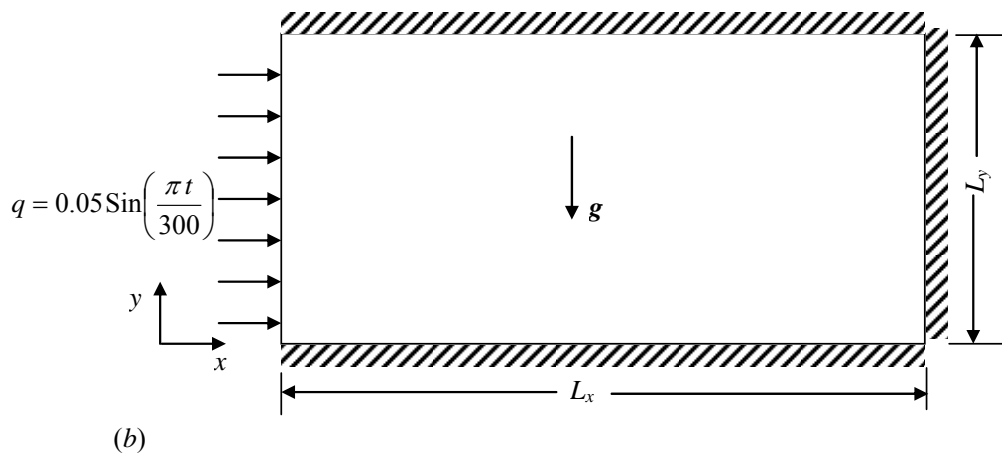


Fig. 5b

CHAPTER 4

MATHEMATICAL FORMULATION

Based on the assumptions discussed in the above section, the reformulated governing equations based on the enthalpy based FG approach are given as follows:

Continuity Equation:

$$\frac{\partial u}{\partial x} + \frac{\partial v}{\partial y} = 0 \quad (1a)$$

x-Momentum Equation:

$$\frac{\partial u}{\partial t} + u \frac{\partial u}{\partial x} + v \frac{\partial u}{\partial y} = -\frac{\partial P}{\partial x} + \nu \left(\frac{\partial^2 u}{\partial x^2} + \frac{\partial^2 u}{\partial y^2} \right) + S_u \quad (1b)$$

y-Momentum Equation:

$$\frac{\partial v}{\partial t} + u \frac{\partial v}{\partial x} + v \frac{\partial v}{\partial y} = -\frac{\partial P}{\partial y} + \nu \left(\frac{\partial^2 v}{\partial x^2} + \frac{\partial^2 v}{\partial y^2} \right) + g\beta(T - T_m) + S_v \quad (1c)$$

Energy Equation:

$$\frac{\partial H}{\partial t} + u \frac{\partial H}{\partial x} + v \frac{\partial H}{\partial y} = \frac{K}{\rho} \left(\frac{\partial^2 T}{\partial x^2} + \frac{\partial^2 T}{\partial y^2} \right) \quad (2)$$

The source terms S_u and S_v are the porosity source terms in the x - and y - momentum equations. It is a term that switches off the velocity as the local liquid fraction closes to zero. These source terms forces the momentum equation to mimic a Darcy equation [14] in the phase change region. The well known Carman-Kozeny equation [15] is used for calculating these porosity source terms. It is given as

$$S_u = -Au \quad \text{and} \quad S_v = -Av \quad (3a)$$

where,

$$A = K_o \frac{(1-f)^2}{(f^3 + q)} \quad (3b)$$

where K_o is a morphology constant and is set to 10^6 for this problem. The constant q is set to 0.001. It is added in the denominator to avoid division by zero. The liquid fraction f can be calculated as

$$f = \frac{\Delta H}{L} \quad (3c)$$

In the energy equation (Eq. 2), the total enthalpy, H is given as

$$H = CT + \Delta H \quad (4)$$

where, ΔH is the enthalpy content or the latent heat content which takes care of the front position at any time instant. The first term in the above equation (Eq. 4) is the sensible heat content. Using Eq. (4), Eq. (2) can be rewritten as

$$\frac{\partial T}{\partial t} + u \frac{\partial T}{\partial x} + v \frac{\partial T}{\partial y} = \alpha \left(\frac{\partial^2 T}{\partial x^2} + \frac{\partial^2 T}{\partial y^2} \right) + S \quad (5a)$$

Where, the source term S in the energy equation is given as

$$S = -\frac{1}{C} \left[\frac{\partial(\Delta H)}{\partial t} + \frac{\partial}{\partial x}(u\Delta H) + \frac{\partial}{\partial y}(v\Delta H) \right] \quad (5b)$$

In the above equation (Eq. 5b), the last two terms are the convective part of the source term due to liquid metal velocity. Since in the present problem, isothermal phase change is considered, hence due to step change in ΔH along with zero velocity at the solid-liquid interface, the convective part of this source term takes the value zero. Hence the source term in Eq. (5b), can be simplified as

$$S = -\frac{1}{C} \frac{\partial(\Delta H)}{\partial t} \quad (5c)$$

Equation (5a) is valid in the whole domain: solid, liquid and the solid-liquid interface. Basically, ΔH is constant in the pure solid and liquid zone. As a result, the source term will be zero in the

pure liquid and solid zones. So, the energy equation (Eq. 5a) reduces to the conventional energy equation for respective phases. Equation (5a) satisfies the interface condition (the Stefan condition) at the interface. How it satisfies the interface condition, interested readers may refer to the work of Shamsundar and Sparrow [16].

The boundary and initial conditions for the present problem are given as follows:

$$T(x, y, 0) = 0 \text{ K}; \quad t = 0, 0 \leq x \leq L_x, 0 \leq y \leq L_y \quad (6a)$$

$$\frac{\partial T(x, y, t)}{\partial \hat{n}} = 0; \quad t > 0, x = L_x, y = 0, L_y \quad (6b)$$

$$T(0, y, t) = 15 \text{ Sin}\left(\frac{\pi t}{300}\right); \quad t > 0, x = 0, 0 \leq y \leq L_y \quad (6c)$$

$$-K \frac{\partial T(0, y, t)}{\partial x} = q = 0.05 \text{ Sin}\left(\frac{\pi t}{300}\right); \quad t > 0, x = 0, 0 \leq y \leq L_y \quad (6d)$$

Equation (6c) is valid for temperature boundary condition and Eq. (6d) is valid for flux boundary condition. An iterative update procedure to update the enthalpy content (ΔH) is briefly described in the next section.

Procedure to Update ΔH

The latent heat content ΔH is updated iteratively in a control volume P [12] as

$$\Delta H^{n+1} = \Delta H^n + \lambda a_p \frac{C \Delta t}{\Delta V_p} (T_p^n - T_{pc}) - 2\varepsilon a_p \lambda \frac{C \Delta t \Delta H^n}{\Delta V_p L} - a_p \varepsilon \lambda \frac{C \Delta t}{\Delta V_p} \quad (7)$$

Where, λ is the under-relaxation factor. This factor is introduced to compensate for the effect of neighboring control volume's change in temperature between two consecutive iterations, n and $n + 1$ which is neglected while deriving the above equation. This assumption is not going to affect the final solution as when the solution converges, temperature between two consecutive iterations remains same. The term a_p is the coefficient of the finite volume discrete equation. The above equation is derived based on the control volume analysis as in the present work, the finite volume method [17] is used to discretize the governing equation. Equation (7) is used to update ΔH at each iteration in a given time step. To avoid overshooting and undershooting problem during computation, the value of ΔH is set to L if $\Delta H > L$ and is set to zero when $\Delta H < 0$. A control volume can be said to melt completely when, $\Delta H = L$ and is said to be solidified completely when $\Delta H = 0$. Thus it can implicitly capture the melting and solidification fronts in the domain at any time instant. In the next section, the numerical method used to solve the above set of governing differential equations (Eqs. 1a - 2) is briefly described.

Numerical Method

The finite-volume method (FVM) of Patankar [17] is used to solve the governing continuity, momentum and energy equations. A brief description of the major features of the FVM used is given here. The detailed discussion of the FVM is available in Patankar [17]. In the FVM, the domain is divided into a number of control volumes such that there is one control volume surrounding each grid point. The grid point is located at the center of a control volume. The governing equation is integrated over each control volume to derive an algebraic equation containing the grid point values of the dependent variable. The discretized algebraic equation for each control volume P is

$$a_P \phi_P = a_P^o \phi_P^o + a_W \phi_W + a_E \phi_E + a_N \phi_N + a_S \phi_S + S_C \Delta V_P \quad (8a)$$

where the coefficient a_P is given as

$$a_P = a_P^o + a_W + a_E + a_N + a_S + S_P \Delta V_P \quad (8b)$$

In Eqs. (8a-b), ϕ is the variable to be evaluated in each control volumes, a is the coefficient of the discretization equation, ΔV is the volume of the control volume and the terms S_C and S_P represents the source terms of the discretization equation. The subscripts W , E , N and S in Eqs. (8a-b) represents respectively the neighboring control volumes at west, east, north and south of the control volume P . The discretization equation then expresses the conservation principle for a finite control volume just as the partial differential equation expresses it for an infinitesimal control volume. The resulting solution implies that the integral conservation of energy is exactly satisfied for any control volume and of course, for the whole domain. The resulting algebraic equations are solved using a line-by-line Tri-Diagonal Matrix Algorithm. The SIMPLER algorithm of Patankar [17] is used to solve the momentum equations. The tolerance limit for convergence of the iterative solution is set to 10^{-11} .

The Overall Solution Procedure

The overall solution procedure for the present FG method can be summarized as follows:

1. Discretize the domain.
2. Set the initial temperature as T_o in the domain.
3. Initially set ΔH to 0 in the domain.
4. Advance the time step to $t + \Delta t$.
5. Calculate the source terms S_u , S_v and S in the x -momentum, y -momentum and the energy equation (Eq. 5a). Also calculate the buoyancy term in the y -momentum equation.
6. Solve Eqs. (1a-1c) for u and v and Eq. 5a for the temperature T .
7. Update the ΔH in the current iteration using Eq. (7).
8. Check for convergence.
 - a) If the solution has converged, then check if the required number of time steps has been reached. If yes, stop. If not, repeat (4) to (7).
 - b) If the solution has not converged, then repeat steps (5) to (7).

CHAPTER 5

MODEL VALIDATION:

To validate the above mathematical model we solve a sample problem with proven results. By this way we can ensure that the results are correct. The following problem is considered and is validated with the problem solved by Hsieh and Choi[8]

PROBLEM DESCRIPTION:

Two examples are used to show the temperature distribution, heat exchange, and interface positions in a phase-change material imposed with cyclic temperature given as

$$F(t) = 932 + 200\sin\left(\frac{\pi}{10}t\right) (K) \quad (1)$$

where the period is 20 s. Aluminum is again used for tests, which has a Stefan number (cT_s/L) of 2.27. Only one cycle is tested for both examples, and the time step used is taken to be 0.05 s.

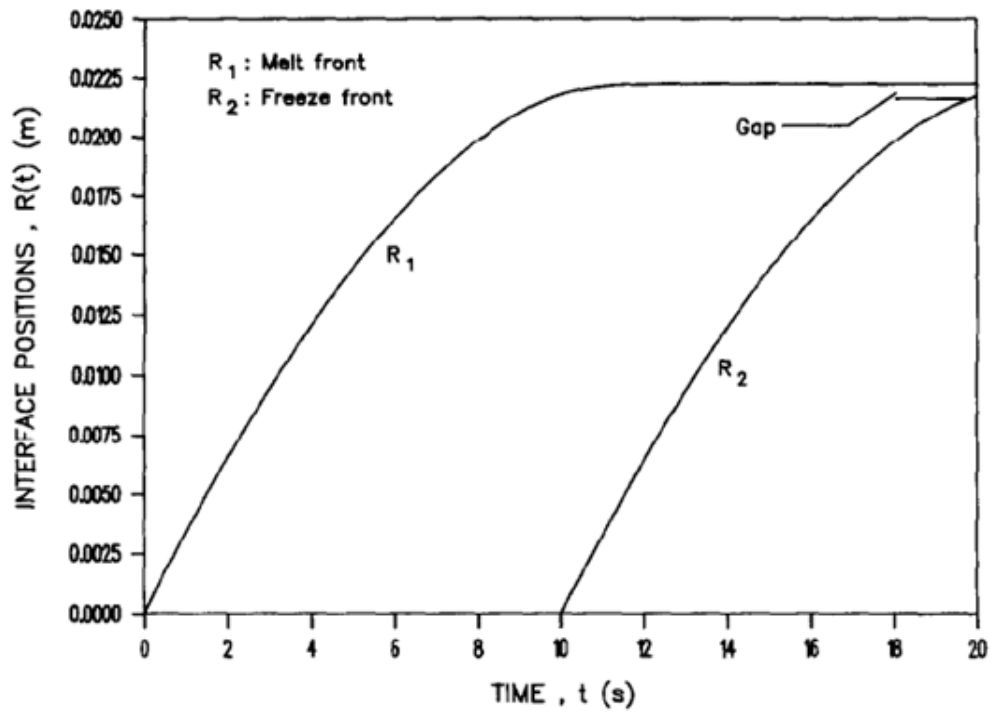
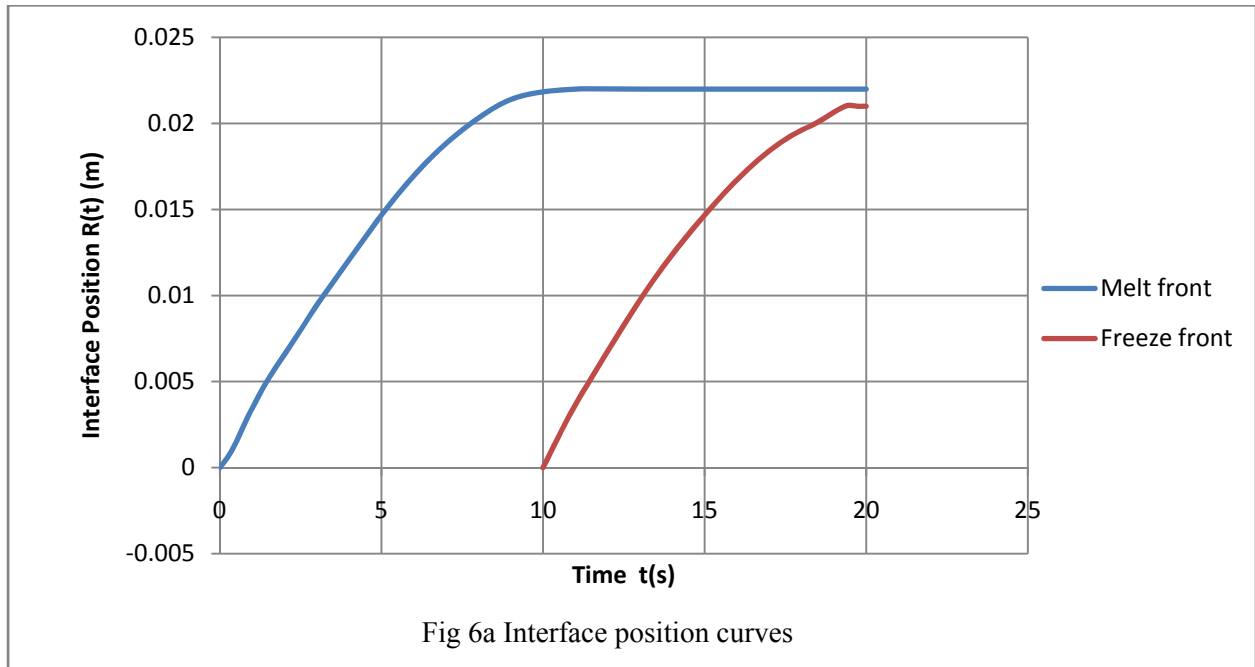
RESULTS AND DISCUSSION

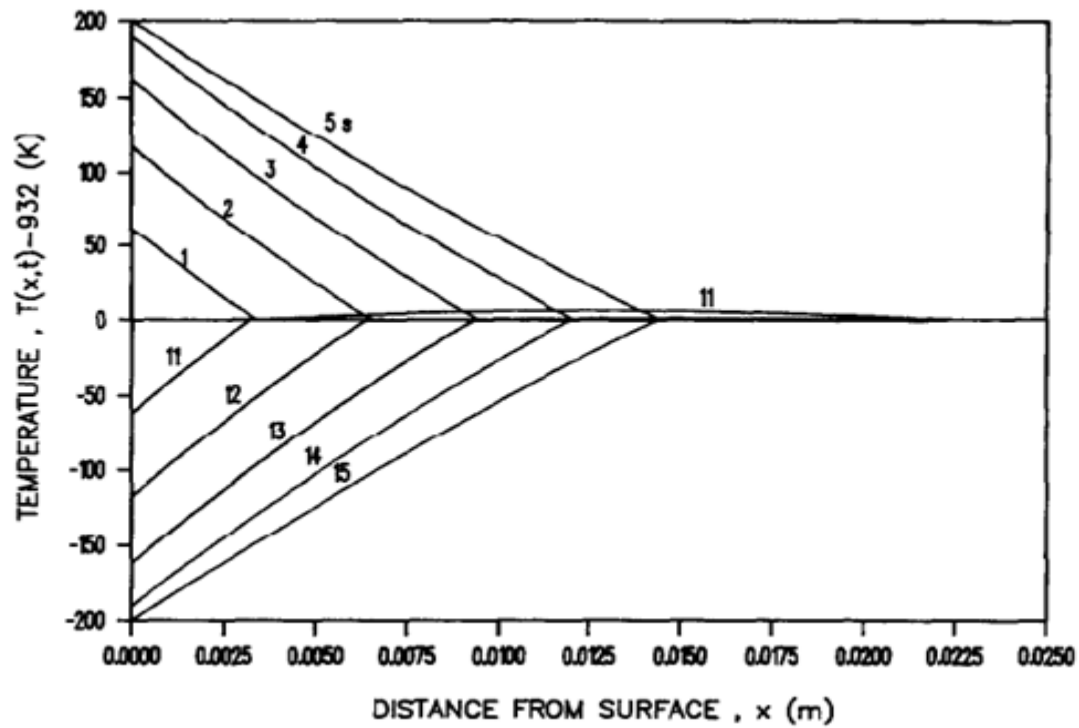
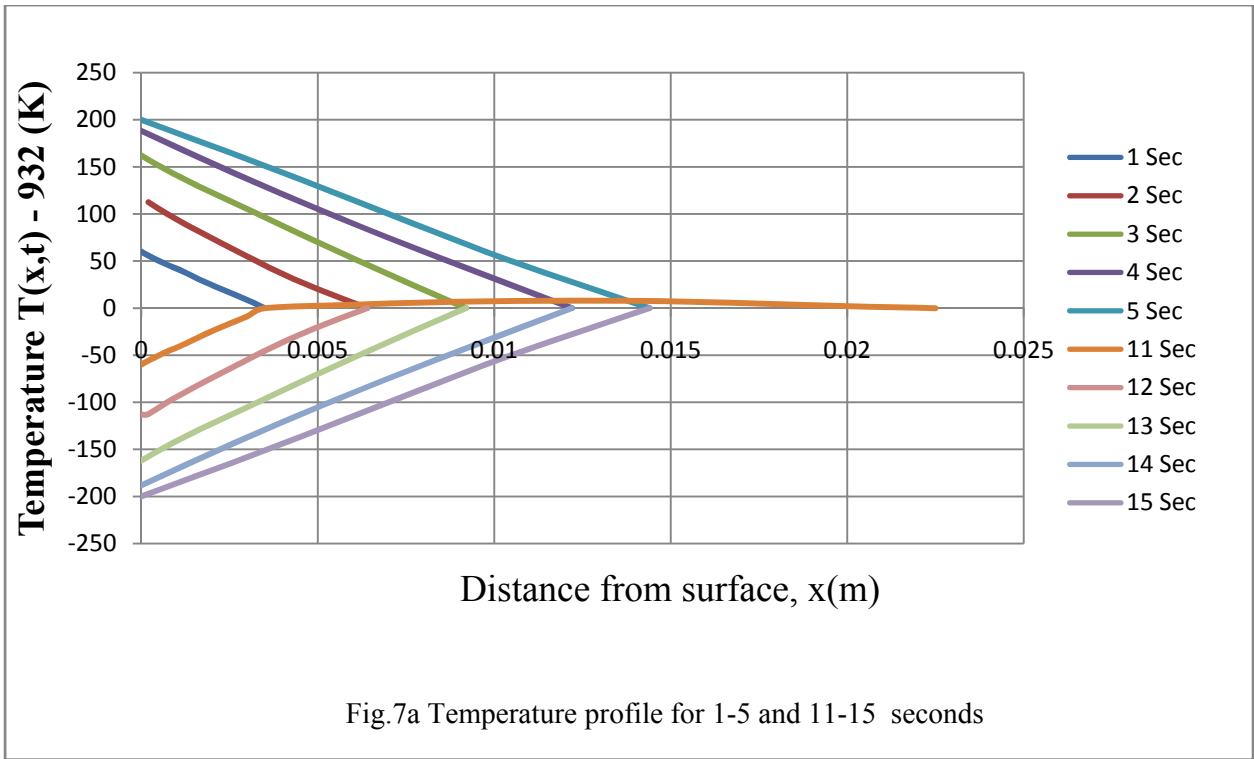
Cyclic temperature condition

The Fig. 6b, 7b and 8b are the results by Hsieh and Choi[8] and the Fig. 6a, 7a and 8a are the results obtained by the present mathematical model. The interface positions for the cyclic temperature condition are plotted in Fig. 3a and Fig. 3b. In Fig 3b two curves are shown; R_1 represents the melting front, while R_2 represents the freezing front. A close examination of these curves shows that the melting front continues to advance even though the surface starts to re-freeze. This can be ascribed to the fact that R_1 is stationary only when the slope of the temperature curve at the melt front is zero. This slope, however, is not zero, as will be shown later. Another point of interest is that if the R_2 curve is moved horizontally to the left so that it matches the R_1 curve at the origin, then the R_2 curve would lie right underneath the R_1 curve, signifying that the freeze front lags slightly behind the melt front..

The temperature profiles in the aluminum are shown in Figs. 4 and 5. Figure 4 covers times from 1 to 5 s and 11 to 15 s. It is noted that, in these figures, the interface positions can be identified

by locating the point of intersection of the curves with the x axis at zero temperature.





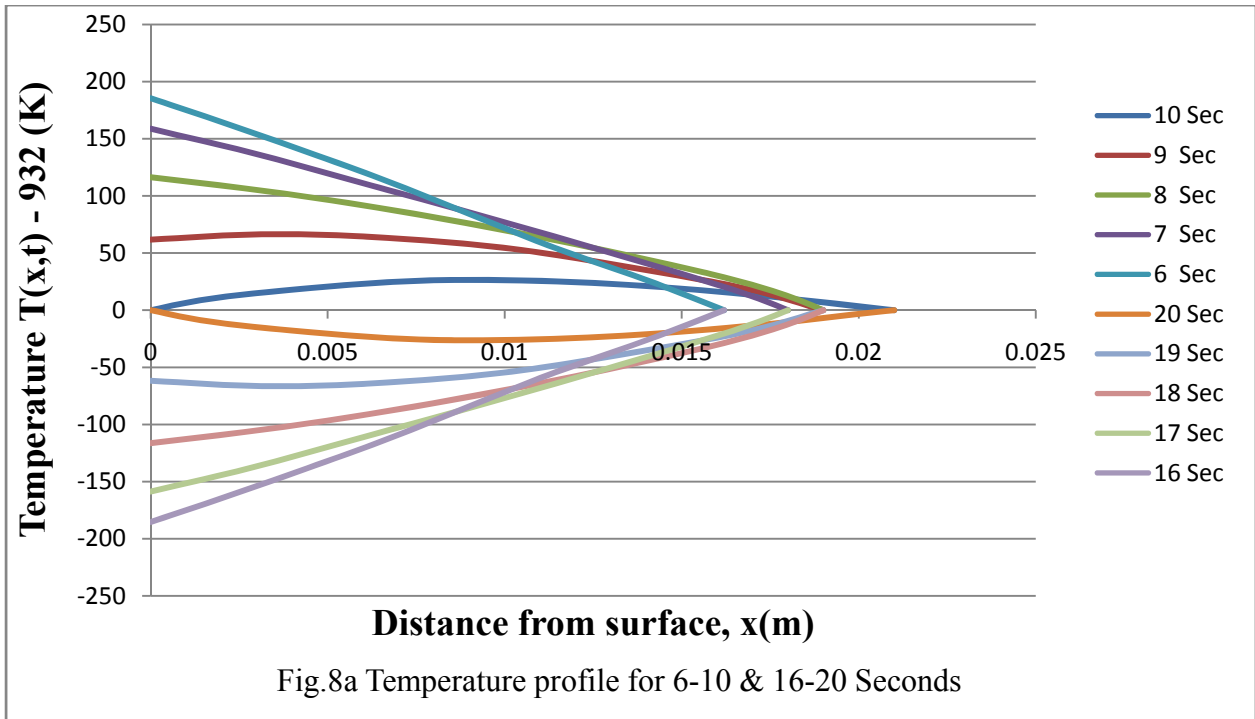


Fig.8a Temperature profile for 6-10 & 16-20 Seconds

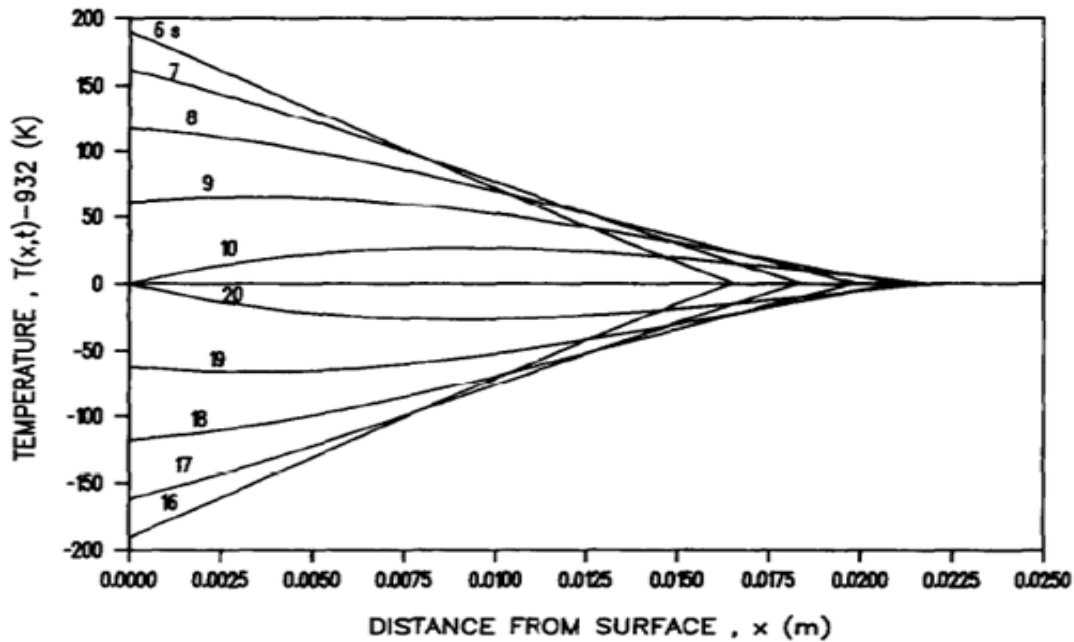


Fig.8b Temperature profile for 6-10 & 16-20 Seconds by Hsieh and Choi[8]

The deviation from the results published by Hsieh and Choi [8] is less than 5% at all conditions. The errors present however is due to the variation in the properties of the material chosen. Hence the model is validated.

CHAPTER 6

RESULTS AND DISCUSSIONS:

The melting and solidification of a gallium-tin (eutectic) alloy is chosen here for study. The Phase change temperature is $T_{pc}=286.75$ (k), the solidous temperature $T_s=282.2$ (K) and the liquidous temperature $T_l=291$ (K). The phase chang temperature T_{pc} is set to zero for presentation of results. The rectangular gallium cavity dimensions are taken as $L_x = 0.089$ m and $L_y = 0.0445$ m. 40×20 control volumes are taken for presentation of results. Although not shown, a grid refinement study is performed and based on this test the above grid size is selected as further refinement does not alter the solution significantly. For presentation of results, the properties of gallium are taken as shown in table 1.

Figure 10 shows the comparison of melt front at 4 time levels with experiment [18] under constant boundary temperature. A good agreement was found between the model predictions and the experiment.

Figure 10 shows the evolution of melting and solidification fronts at different cycles of time during cyclic variation of temperature. The front evolutions in two cycles ($0 \leq t \leq 600$ and $600 \leq t \leq 1200$) are shown. The velocity vectors are shown in the melt region. In the first half of the first cycle, melting occurs and in next half solidification starts for $300 \leq t \leq 600$. Similarly, the next cycle ($600 \leq t \leq 1200$) also follows the same trend of melting and solidification. During melting cycle, the top of the cavity melts more rapidly than the bottom one. This is due to the natural convection effect in the melt region. However, solidification front moves almost like 1-D case. This is because of the rapid dissipation of temperature gradients in the melt. Hence the movement of the solidification front is not modified by the fluid flow. Figure 8 shows the simultaneous melting and solidification front evolution under cyclic variation of heat flux. Similar phenomenon is observed as found in cyclic temperature boundary condition. However, in cyclic flux variation, the melting and solidification fronts moves relatively faster which can be clearly seen by comparing Fig. 10 and Fig11. This is due to the rapid addition and removal of heat in the cycle operation.

Figure 12 shows the cyclic variation of temperature at the center of the left boundary imposed with cyclic variation of heat flux. The maximum and minimum temperature is found to 26.624 K and -87.314 K. Because of some phase shift, the periodic variation of temperature is not exactly as that of heat flux variation. Figure 13 shows the temperature variation at the left boundary at different cycles of time. It is found that, the temperature almost constant in the solidification cycle. This is the reason that the solidification front takes a regular shape compared to the melt front.

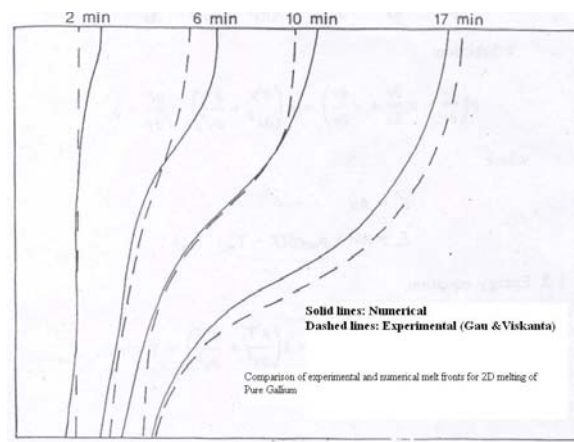


Fig.9. Comparison with experiment for melting of pure gallium [18].

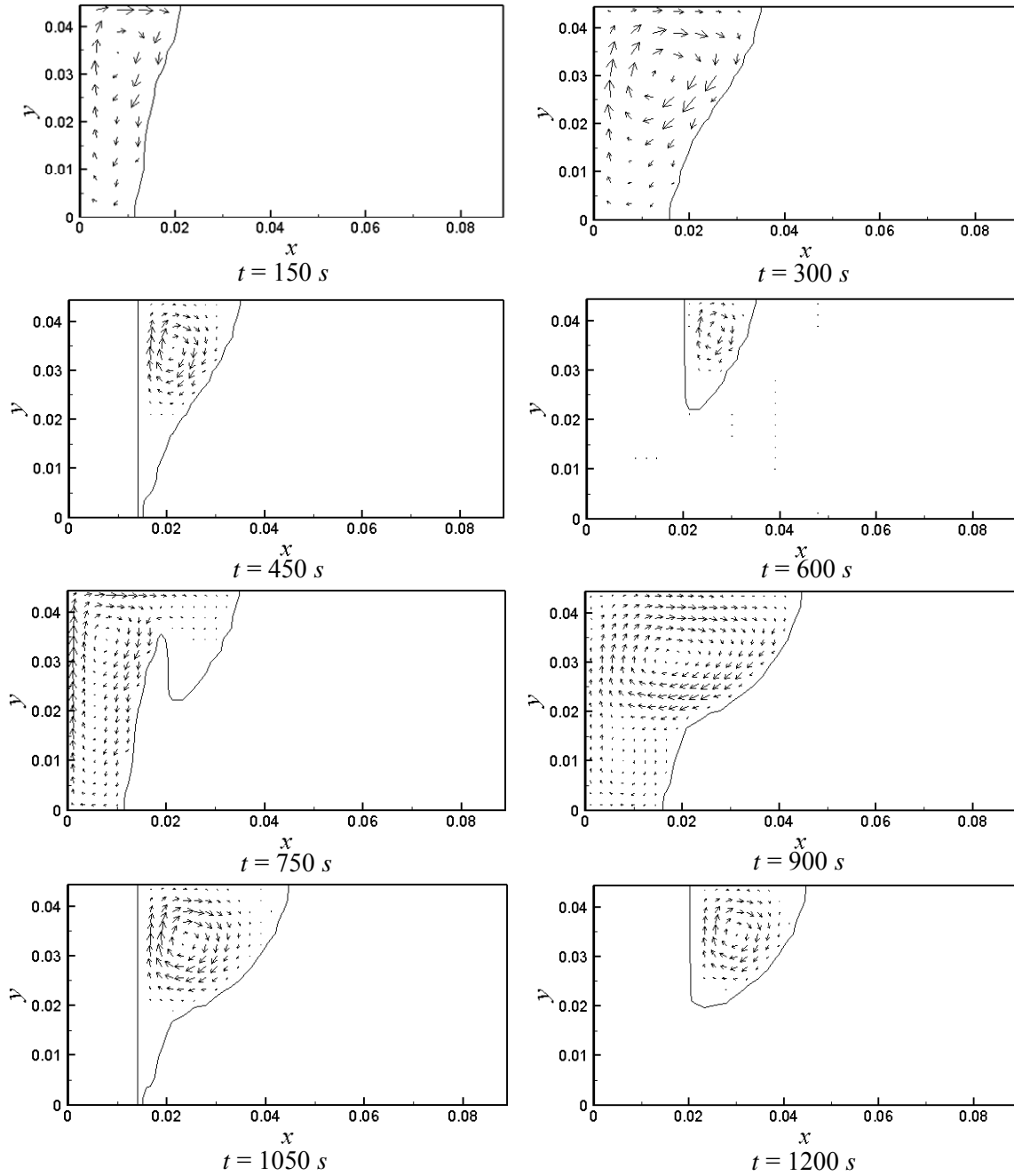


Figure10. melting and solidification front positions and velocity vectors in the melt region at different time instant in two cycles during cyclic variation of temperature.

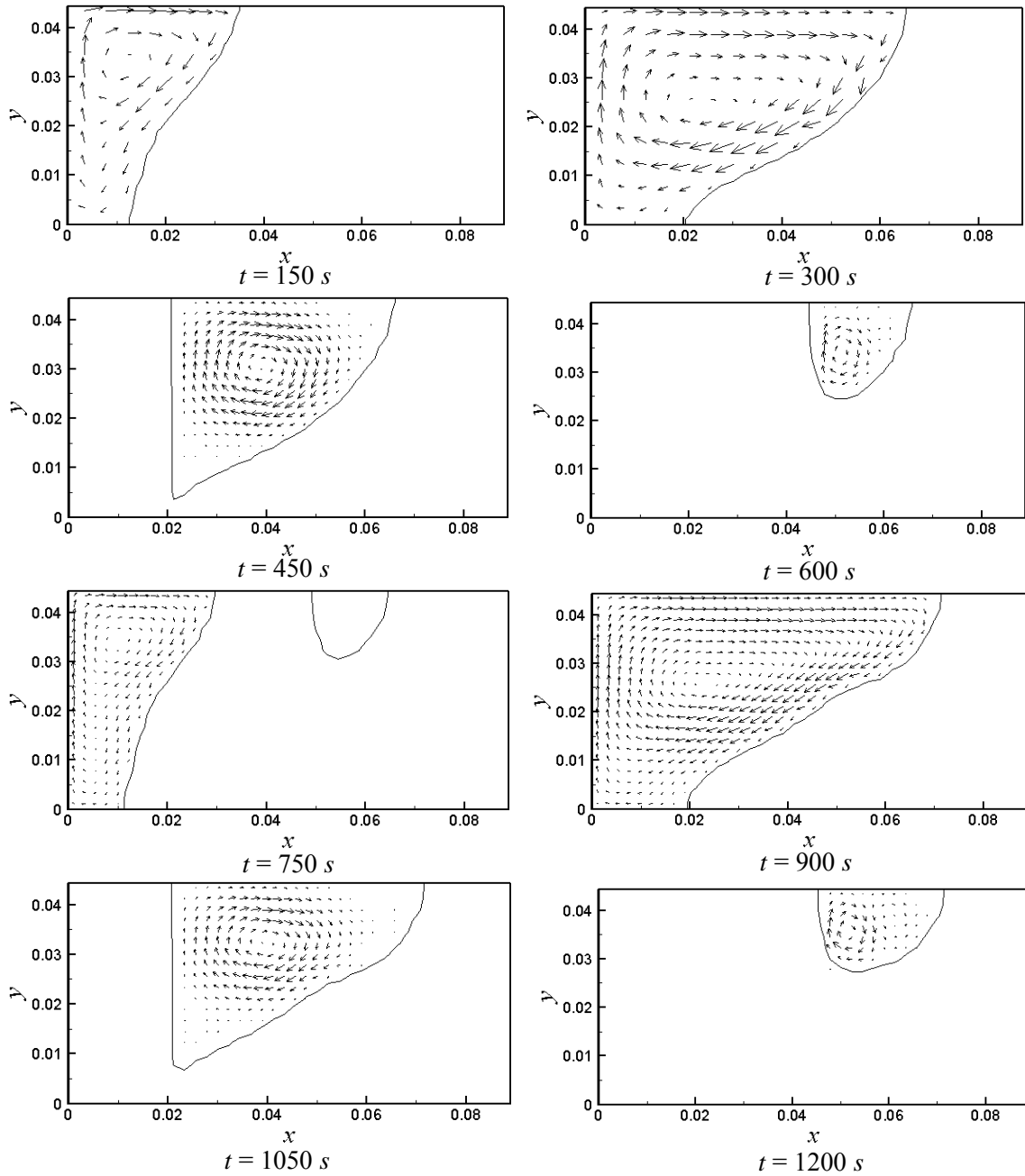


Figure11. melting- and solidification front positions and velocity vectors in the melt region at different time instant in two cycles during cyclic variation of heat flux.

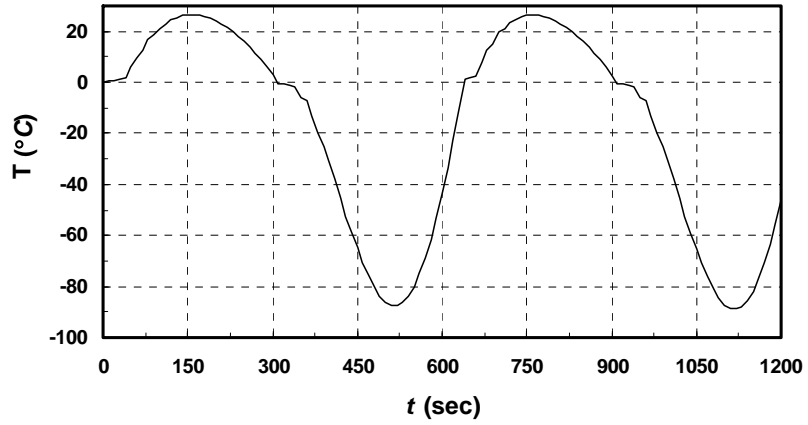


Fig.12 Variation of temperature with time at the center of the left boundary in cyclic heat addition.

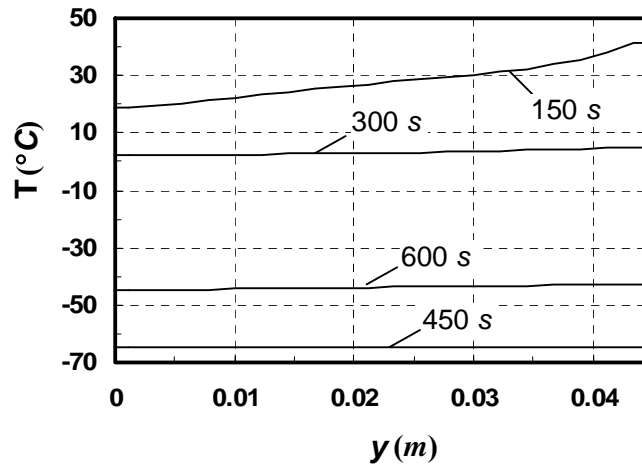


Fig.13. Temperature variation at the left boundary during cyclic variation of heat flux.

CHAPTER 7

CONCLUSIONS:

Summary:

An enthalpy based fixed-grid method is presented for modeling simultaneous melting and solidification of rectangular gallium-tin alloy cavity under imposed temperature and flux fluctuations in one of the boundaries. Because of the cyclic variation of temperature which cycles above and below the phase change temperature, simultaneous melting and solidification occurs during the cycle operation. Due to natural convection, the melt front takes an irregular shape compared to the solidification front. This can further be clarified by uniform distribution of temperature at the boundary. The solidification front is not affected by the fluid flow due to rapid dissipation of heat in the melt.

Future scope:

The solution to these types of problem can be further improved upon by considering the change of the thermal diffusivity constant in different phases, a more general case of melting profile can be used in place of linear phase change. The case can be extended to 3D with complex boundary condition to simulate actual engineering problems.

CHAPTER 8

REFERENCES

1. J. C. Muehlbauer and J. E. Sunderland, *Appl. Mech. Rev.*, **18** (1965), 951-959.
2. T. R. Goodman, *Adv. Heat Transfer*, **1** (1964), 71-79.
3. L. I. Rubinstein, *Am. Math. Soc. Transl. Math. Monogr.*, **27** (1971).
4. J. R. Ockendon and W. R. Hodgkins, *Moving Boundary Problems in Heat Flow and Diffusion*, Clarendon Press, London (1975).
5. D. G. Wilson, A. D. Solomon and P. T. Boggs, *Moving Boundary Problems*, Academic Press, New York (1978).
6. J. Crank, *Free and Moving Boundary Problems*, Clarendon Press, London (1984).
7. L. S. Yao and J. Prusa, *Adv. Heat Transfer*, **19** (1989), 1-95.
8. C-Y Choi and C. K. Hsieh, *Int. J. Heat Mass Transfer*, **35** (1992), 1181-1195.
9. J. L. Duda and J. S. Vrentas, *Chem. Engg. Sci.*, **24** (1969), 461-470.
10. M. Hasan, *PhD Thesis*, University of McGill (1988).
11. Z. X. Gong, Y. F. Zhang and A. S. Mujumdar, *Computational Modeling of Free and Moving Boundary Problems*, CMP, Southampton (1991).
12. A. D. Brent, V. R. Voller and K. J. Reid, *Numerical Heat Transfer*, **13** (1988), 297-318.
13. V. R. Voller, P. Felix and C. R. Swaminathan, *Int. J. Num. Meth. Heat Fluid Flow*, **6** (1996), 57-64.
14. R. Mehrabian, M. Keane and M. C. Flemings, *Met. Trans. B*, **1** (1970), 1209-1220.
15. P. C. Carman, *Trans. Inst. Chem. Engrs.*, **15** (1937), 150-166.
16. N. Shamsundar and E. M. Sparrow, *Journal of Heat Transfer*, **97** (1975), 333-340.
17. S. V. Patankar, *Numerical Heat Transfer and Fluid Flow*, Hemisphere, London (1980).
18. C. Gau and R. Viskanta, *Int. J. Heat Mass Transfer*, **27** (1984), 113-123.
19. C parakash , M Samonds and A.K.Singhal, *Int.J.Heat Mass Transfer*,**30**(1987),2690-2694